Chalcogenide Letters Vol. 22, No. 3, March 2025, p. 197 - 204

Morphological study of bulk sample averse to thin films for a quaternary glassy alloy system

P. Kaushik [a,*], A. Devi [b], H. Singh [a]
[a] *Department of Applied Sciences, The North Cap University, Gurugram, India*
[b] *Department of Applied Sciences, Amity University, Gurugram, India*

The structural properties of bulk as well as thin films of nanostructured $Bi_1Te_{15}Se_{84-x}$ Pb_x ($0 \leq x \leq 8$) glassy alloys has been studied in this paper. Conventional melt quenching method is employed to prepare the samples of $Bi_1Te_{15}Se_{84-x}$ Pb_x ($0 \leq x \leq 8$) alloys. Thin films with thickness of approximately 158nm of the obtained bulk compositions were deposited on dry cleaned glass substrates by thermal evaporation technique. The structural characterization was carried out using XRD and SEM. Energy dispersive X-ray spectroscopy (EDX) indicates that samples are nearly stoichiometric. X-ray diffraction patterns indicate that they are in the crystalline state. SEM study indicates the formation of snow flaky structures with agglomeration with the rise in lead content in the sample. Raman spectroscopy is used to study how changes in composition due to Pb doping affect lattice vibrations and electron-phonon interactions.

(Received November 22, 2024; Accepted February 28, 2025)

Keywords: Chalcogenides, XRD, Crystalline, Morphology, Spectroscopy

1. Introduction

Chalcogenide glasses have been considered broadly since they are great glass formers and have great warm steadiness [1-5].Chalcogenide glasses show optical straightforwardness from unmistakable to infrared locales making them reasonable for utilize in optical magnifiers, infrared imaging and optoelectronic applications Bi-based compounds containing oxides, chalcogenides and halides, such as Bi_2O_3,Bi_2S_3, Bi_2Se_3, graphene/CNT/carbon, etc., are all inclusive cathode materials for utilize in supercapacitors due to their moo fetched, chemical steadiness, mechanical quality, normal wealth, natural invitingness, quasi-faradaic redox responses, and the accessibility of different structures and morphologies. Within the later a long time, work has been done on ternary and parallel nanostructured glasses but work on quaternary nanostructured glasses is still in its early stages. Nanostructured chalcogenide glasses contain of nanometre measured shiny clusters associated by glass-glass interfacing of decreased thickness [6-7]. Over the past few a long time, stage alter optical memory innovation has become one of the foremost profitable highlights of these materials. Stage alter applications works on the reality that by applying warm or a laser pillar, chalcogenide glasses can alter between two basic shapes, nebulous and crystalline. These two shapes can coexist at room temperature. The little distinction in optical reflectivity (~ 20%) between two states of the same fabric is utilized for optical capacity applications. The nebulous nature of chalcogenide semiconductors offers them potential employments in high-density data capacity, high-resolution show gadgets and fabricating optical capacity media that can be deleted. Within the show paper we have examined the auxiliary properties of $Bi_1Te_{15}Se_{84-x}$ Pb_x ($0 \leq x \leq 8$) bulk test as well as lean movies arranged by dissolve extinguishing and warm vanishing procedure separately. In this composition Se is utilized as major constituent since of its broad applications in electronic and optoelectronic device materials. The composition $Bi_1Te_{15}Se_{84-x}$ Pb_x is chosen as base composition because it has obvious optical, electrical and warm properties [8]. Diverse properties

* Corresponding author: pkaushik520@gmail.com
https://doi.org/10.15251/CL.2025.223.197

such as electrical, optical and stage change considers of Se-Te-Bi glasses have been investigated by different analysts [9-12]. The expansion of a metallic added substance, like lead, to a ternary chalcogenide changes the populace of emphatically and contrarily charged valence modification sets, which at that point influences the properties of this composition [13-14]. Chalcogenide glasses have a place to an curiously bunch of materials owing to their tunable electrical and optical properties. The undefined structure of the glasses permits the alter in structure taking after a slight change in composition as well as the temperature. The addition of debasements in these frameworks leads to abandons within the structure which presents limited states within the versatility hole [15-20]

2. Experimental techniques

$Bi_1Te_{15}Se_{84-x}$ Pb_x ($0 \leq x \leq 8$) chalcogenide bulk sample has been prepared using the conventional melt quenching technique. The raw materials obtained are manufactured by Fischer company with 99.99% purity. High purity (5N) materials were weighed using a digital weighing balance with a least count of 0.5 gm, according to their atomic weight percentage and sealed in quartz ampoules in a vacuum of 10^{-4} torr. The ampoules were placed inside a furnace that is heated at a rate of 2-3 degrees celsius per minute until the temperature 1000 degrees celsius is attained. In order to make the sample homogeneous, the process of shaking the samples at regular interval is done. Ice-cold water is used to quench the bulk sample.

In order to prepare the thin films, a glass substrate that which has been cleaned with a soap solution, then ultrasonically cleaned with acetone. The vacuum evaporation technique is utilized to prepare thin films at room temperature and a low pressure of 10^{-4} torr. The sample was kept in a molybdenum boat and the substrate was held at normal depth on the boat. The thickness of the films was measured using a quartz crystal monitor, which was placed at the same height as the substrate. The crystalline nature of the films was confirmed by x-ray diffraction, with peaks appearing in the spectra.

3. Results and discussions

3.1. Energy-dispersive X-ray spectroscopy (EDX)

The elemental characterization of the surface of the samples was investigated by EDX. The elements included in the composition of the sample are shown in Table 1 in the form of mass and atomic percentages.

Table 1. (EDX mass and atomic percentage for different concentrations).

Chalcogenide glass **$Bi_1Te_{15}Se_{84-x}$ Pb_x**	Bismuth		Tellurium		Lead		Selenium	
	Mass (%)	Atomic (%)	Mass (%)	Atomic (%)	Mass (%)	Atomic (%)	Mass (%)	Atomic (%)
X=2	3.06 ±0.71	1.32±0.31	26.28±1.03	18.55±0.73	0.66 ±0.61	0.29 ±0.27	69.99 ±1.53	79.84±1.75
X=4	2.48 ±0.50	1.07 ±0.22	28.09 ±0.83	19.91 ±0.59	0.74 ±0.47	0.32 ±0.20	68.70 ±1.21	78.70±1.38
X=6	1.64 ±0.52	0.74 ±0.23	22.39 ±0.64	16.44 ±0.47	9.98 ±0.61	4.51 ±0.28	65.99 ±0.97	78.31±1.16
X=8	5.96 ±1.96	2.93 ±0.96	35.46 ±2.53	28.51 ±2.03	9.36 ±2.02	4.63 ±1.00	49.22 ±3.04	63.93±3.94

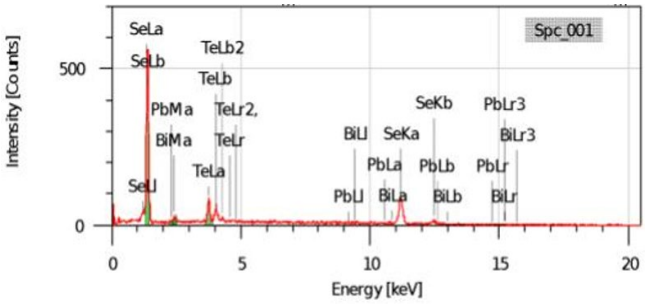

Fig. 1. (EDX Spectrum for x=2).

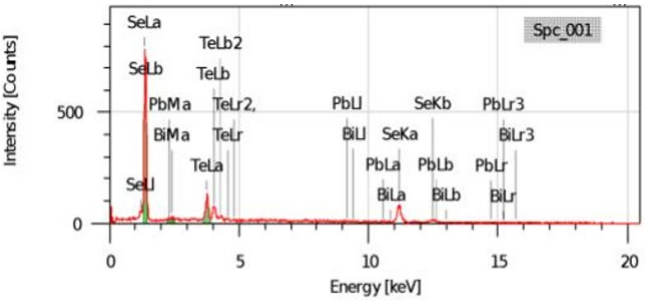

Fig. 2. (EDX Spectrum for x=4).

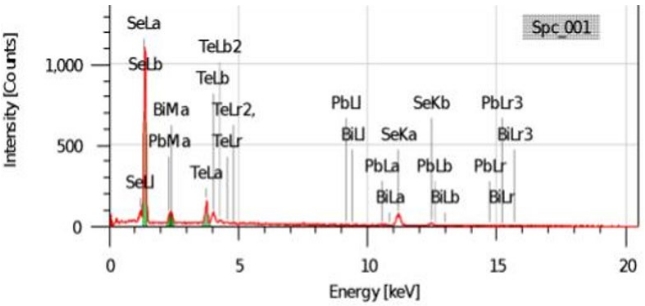

Fig. 3. (EDX Spectrum for x=6).

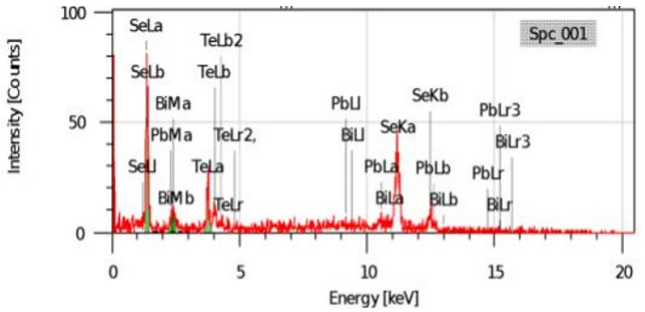

Fig. 4. (EDX Spectrum for x=8).

3.2. Field-Effect Scanning Electron Microscope (FESEM)-

The topography of the surface of the bulk sample as well as the thin films is investigated using JEOL FESEM (JSM-IT200) model, which allows high magnification and precision imaging of the surface of the materials. The left side images in Figure 5,6,7,8 is the FESEM images of the bulk sample and the right-side images in Figure 5,6,7,8 are for thin films. From the FESEM image, it is noted that snowy flakes and rocky structures are formed which are of the order of few nanometres to few micrometres in size. It is also observed that with an increase in the concentration

of Pb, the shape of the particles gets distorted and agglomeration could also be seen. With the increase in x the snowy flaky structures are observed to change to rocky structures.

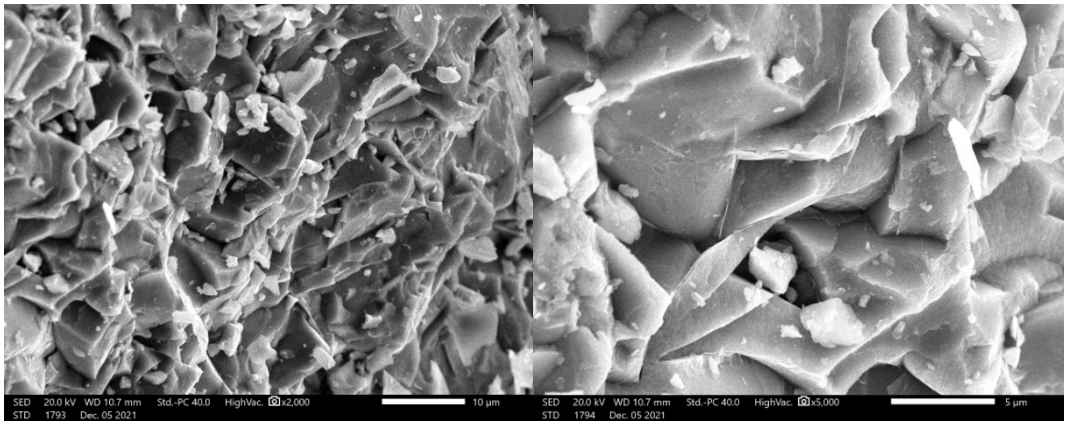

Fig. 5 (FESEM images for x=0):(Left side) Alt Text: Showing Scanning electron microscopy image of the bulk sample for x=0; (Right side) Alt Text: Showing Scanning electron microscopy image of the thin film for x=0.

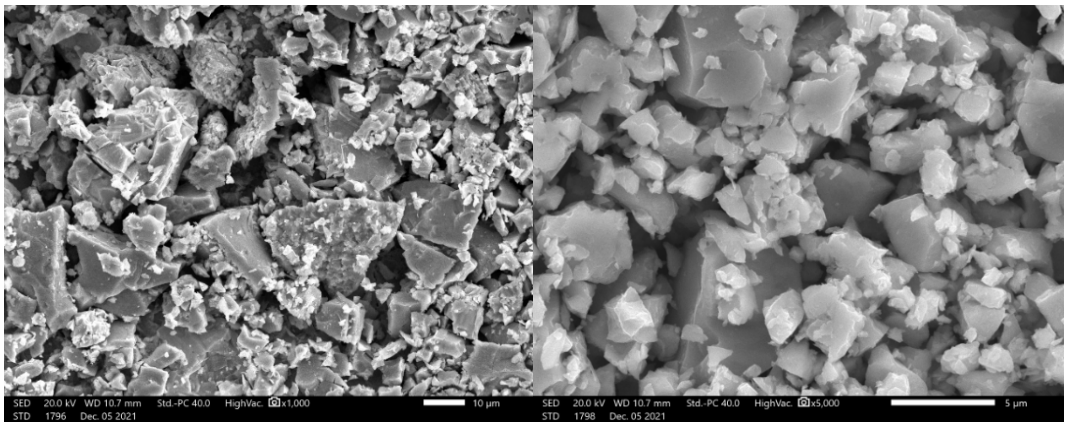

Fig. 6 (FESEM images for x=4): (Left side) Alt Text: Showing Scanning electron microscopy image of the bulk sample for x=4; (Right side) Alt Text: Showing Scanning electron microscopy image of the thin film for x=4.

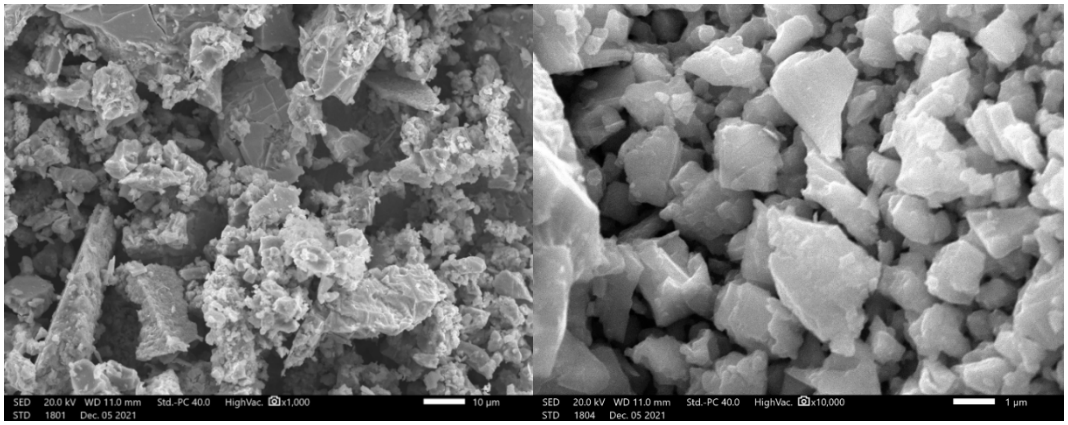

Fig. 7 (FESEM images for x=6): (Left side) Alt Text: Showing Scanning electron microscopy image of the bulk sample for x=6; (Right side) Alt Text: Showing Scanning electron microscopy image of the thin film for x=6.

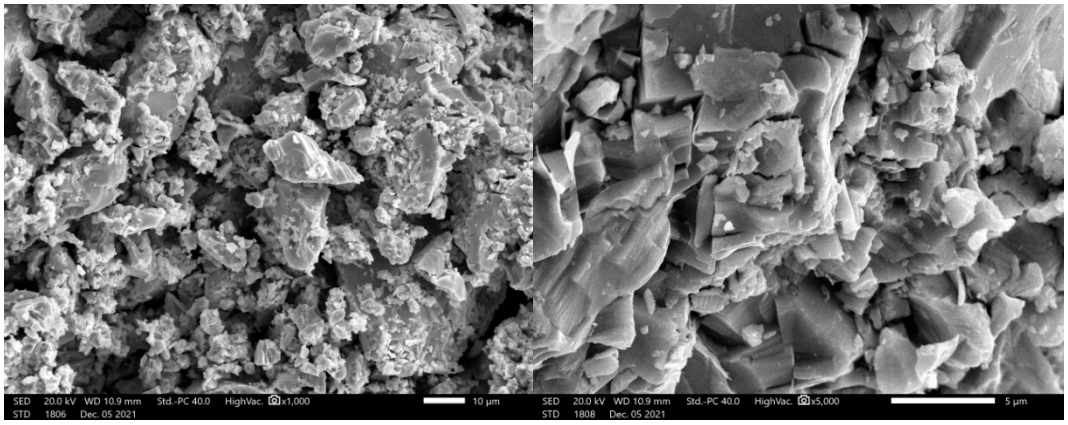

Fig. 8. (FESEM images for x=8): (Left side) Alt Text: Showing Scanning electron microscopy image of the bulk sample for x=8; (Right side) Alt Text: Showing Scanning electron microscopy image of the thin film for x=8.

3.3. X-Ray Diffraction

X-ray diffraction of the samples was performed using X-ray diffractometer with Cu-Kα source(λ=1.54Å). The diffractogram of pure $Bi_1Te_{15}Se_{84-x}$ Pb_x is shown in figure 9. It is perceived that the pure sample is amorphous in nature with one peak at 29.5º of (110) (Table 2) and smaller peak at 23.4º of (100) crystal plane of $Bi_1Te_{15}Se_{84-x}$. For other samples, distinct peaks are observed at various points. With the incorporation of Pb, one characteristic peak is observed at 29.5º along with other peaks indicating the formation of new phase. With an increase in the concentration of Pb, the intensity of the existing phase is enhanced as the intensity of the peak is increased. The presence of various peaks in the XRD graph confirms the crystalline nature of the sample.

Table 2. (XRD analysis for different concentrations).

2 Θ (degrees)	Θ in radians	Sin Θ	Sin^2 Θ	hkl	d (Å)
29.50	0.26	0.25	0.06	110	3.03
23.46	0.20	0.20	0.04	100	3.85
29.44	0.26	0.25	0.06	111	3.08
23.53	0.20	0.20	0.04	010	3.85
29.40	0.26	0.25	0.06	011	3.08

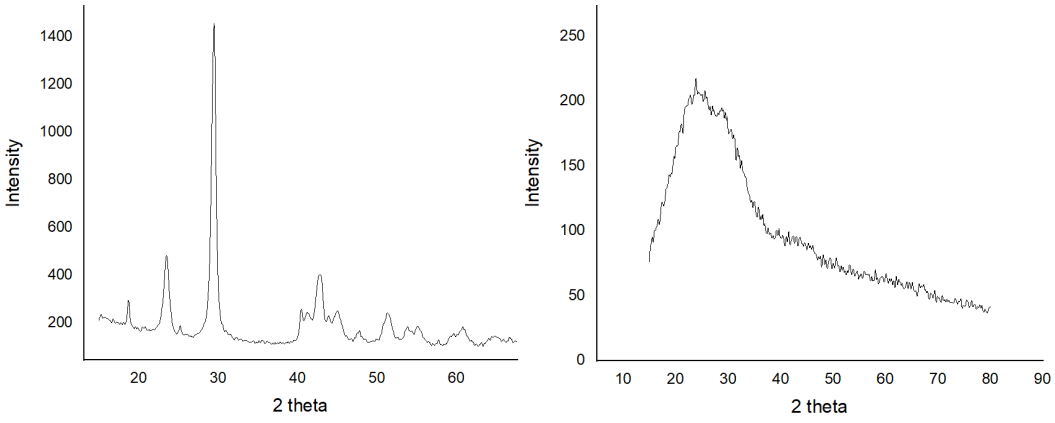

Fig. 9. (XRD Patterns for x=0 bulk sample and thin films): (Left side) Alt Text: Showing X-ray diffraction image of the bulk sample for x=0 (Crystalline nature); (Right side) Alt Text: Showing X-ray diffraction image of the thin film for x=0 (Amorphous nature).

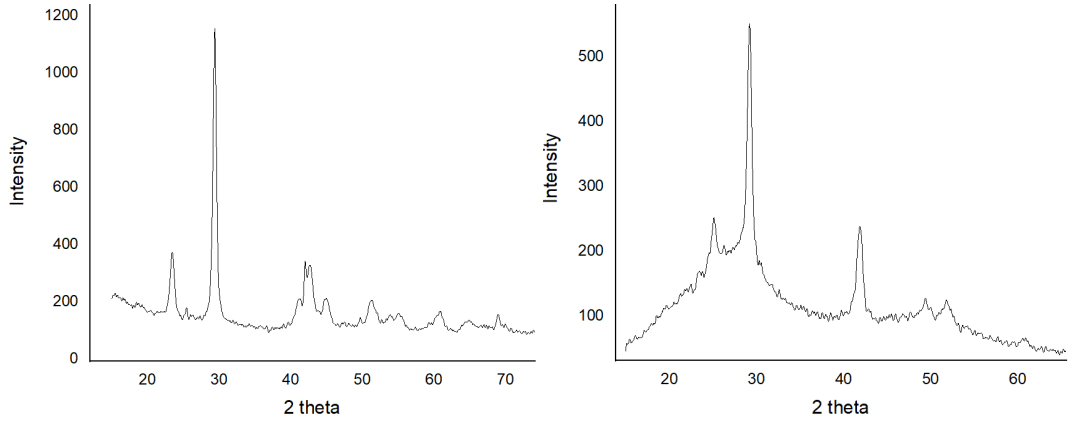

Fig. 10 (XRD Patterns for X=2 bulk sample and thin films): (Left side) Alt Text: Showing X-ray diffraction image of the bulk sample for x=2 (Crystalline nature); (Right side) Alt Text: Showing X-ray diffraction image of the thin film for x=2 (Crystalline nature).

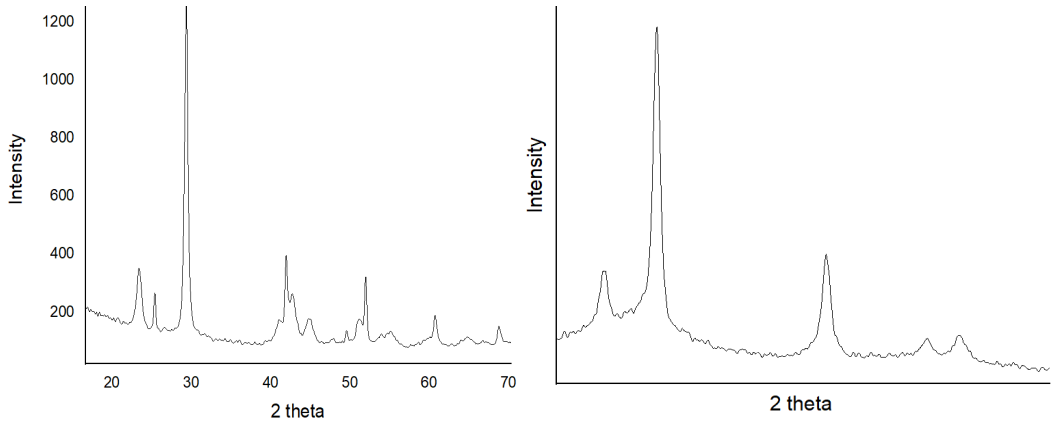

Fig. 11. (XRD Patterns for X=4 bulk sample and thin films): (Left side) Alt Text: Showing X-ray diffraction image of the bulk sample for x=4 (Crystalline nature); (Right side) Alt Text: Showing X-ray diffraction image of the thin film for x=4 (Crystalline nature).

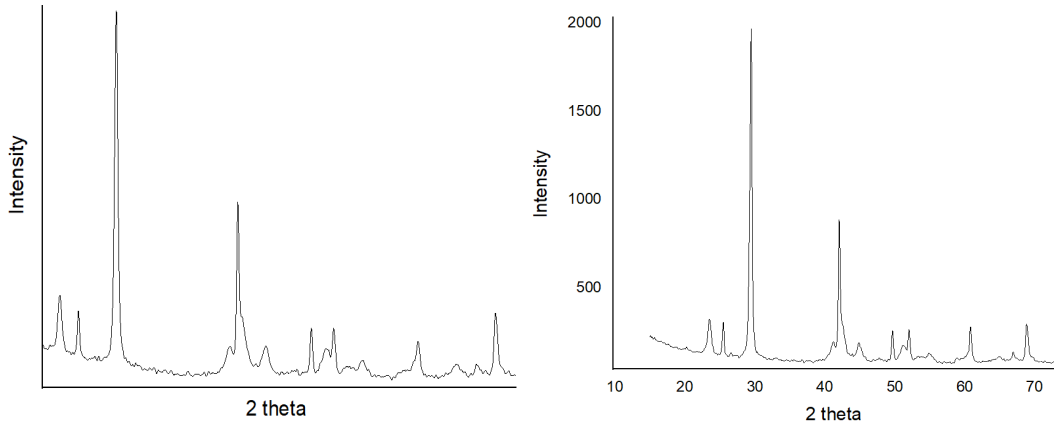

Fig. 12. (XRD Patterns for X=6 and X=8 bulk samples): (Left side) Alt Text: Showing X-ray diffraction image of the bulk sample for x=6(Crystalline nature); (Right side) Alt Text: Showing X-ray diffraction image of the bulk sample for x=8(Crystalline nature).

3.4. Raman Spectroscopy

The use of Raman spectroscopy allows for the analysis of materials in detail, as the spectroscopy is very sensitive to changes in the electronic structure. Secondary phases can be detected by using the technique. The intensity of Raman scattering from a crystal can be strongly related to the structure and orientation of the light that is incident on it and the scattered light. In sample x=0, the broad band appears nearly at 82.8 cm^{-1}. This may be due to the mixed contribution of Te-Bi and Se-Bi modes. With the addition of Pb in the sample, the broad band appears almost at the same position.

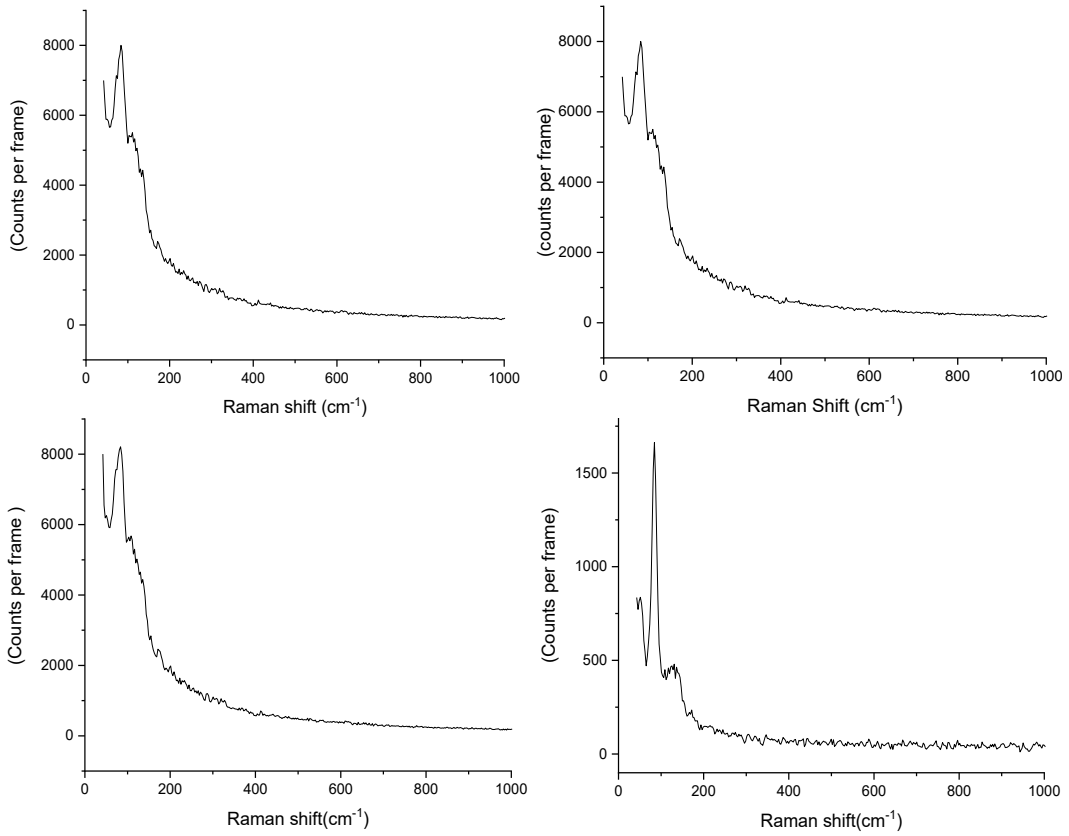

Fig. 13. Raman Spectra of bulk system for various values of x: Alt Text: Showing Raman Spectroscopy images of the bulk sample for x=2,4,6,8.

4. Conclusion

In a nutshell, pure $Bi_1Te_{15}Se_{84-x}Pb_x$ and its thin films are fabricated using the melt quenching technique and thermal evaporation technique. The prepared pure thin film is amorphous while other samples are crystalline in nature. The elemental analysis of all samples is investigated using EDS technique and the percentages are close to the ideal elemental constituents. In XRD, the d-spacing which is calculated using the Bragg's relation corresponding to the 29.50º is found to be 3.03 Å. Raman spectroscopy is used to investigate how the compositional variations due to Pb doping effect the lattice vibrations and the electron phonon interaction.

Acknowledgements

We are grateful to the USIC division of Jawaharlal Nehru University for providing us with the characterization facilities.

References

[1] M.A. Majeed Khan, M. Wasi Khan, Mansour Alhoshan, J. Materials Letters (2010);64: 1929-1932; https://doi.org/10.1016/j.matlet.2010.05.033

[2] Deepika, H. Singh, J. Infrared Physics & Technology (2017);85:39-43; https://doi.org/10.1016/j.infrared.2017.05.014

[3] M. S. Kamboj, R. Thangaraj, J. Eur. Phys. J. Appl.Phys. (2003);24: 33-36; https://doi.org/10.1051/epjap:2003052

[4] N.B. Maharjan, D. Bhandari, N.S. Saxena, J. Material Sci. (2000);23:369-376.

[5] S.B. Bhanu Prashanth, S. Asokan, J. Non-Cryst. Solids (2009); 355:164-168; https://doi.org/10.1016/j.jnoncrysol.2008.11.003

[6] J. Jing, A. Kramer, R. Birringer, H. Gleiter, J. Non-Crystalline Solids (1989);113:167-170; https://doi.org/10.1016/0022-3093(89)90007-0

[7] H. Gleiter, J. Nanotechnol. (2013); 4:517-533; https://doi.org/10.3762/bjnano.4.61

[8] A. Sharma, P.B. Barman, J. Physica B: Condens. Matter (2010); 822-827.

[9] N Suri, P K Khanna, R Thangraj, Journal of Optoelectronic Advanced Materials (2009); 794

[10] N Suri, K S Bindra, M Ahmad,J. Applied Physics A (2008), 149; https://doi.org/10.1007/s00339-007-4242-z

[11] H Wang, N Madaan, J A Bagley Diwan, Y Liu, R C Davis, J.Thin Solid Films(2014);124; https://doi.org/10.1016/j.tsf.2014.08.026

[12] M.A Alvi, J. Superlattices and Microstructures (2014);73 1; https://doi.org/10.1016/j.spmi.2014.05.004

[13] A. Sharma, P.B. Barman, J. Philos. Mag. (2010); 2149-2159; https://doi.org/10.1080/14786431003630819

[14] A. Sharma, P.B. Barman, J. Thin Solid Films (2009); 3020-3023; https://doi.org/10.1016/j.tsf.2008.11.123

[15] N.F. Mott, J. Philos. Mag., (1969);835-852; https://doi.org/10.1080/14786436908216338

[16] N.F. Mott, E.A. Davis, J. Philos. Mag (1970),903-922.

[17] N.F. Mott, E.A. Davis, J. Clarendon, Oxford, (1970).

[18] Deepika, H. Singh, J. Nanostruct. Nano-objects, (2017),192.

[19] Deepika, H. Singh, J. MAPAN 33 Metrol. Soc. Ind(2018);165-168; https://doi.org/10.1007/s12647-017-0240-6

[20] Deepika, H. Singh, N.S. Saxena, J. Mater. Res. Express, (2017) 035203.